Ultrasound Characterization of Mechanical Properties of Nanometric Contrast Agents with PLGA Shell in Suspension

François Coulouvrat, Ksenia Astafyeva, Jean-Louis Thomas, Nicolas Taulier, Jean-Marc Conoir, Wladimir Urbach

Ultrasound Characterization of Mechanical Properties of Nanometric Contrast Agents with PLGA Shell in Suspension

F. Coulouvrat[a], K. Astafyeva[b], J.-L. Thomas[c], N. Taulier[b], J.-M. Conoir[a] and W. Urbach[b]

[a]CNRS, Institut Jean Le Rond d'Alembert - UMR CNRS 7190, Université Pierre et Marie Curie - 4 place Jussieu, 75005 Paris, France
[b]Université Pierre et Marie Curie, Laboratoire d'Imagerie Paramétrique, UMR CNRS 7623, 15 rue de l'école de médecine, 75006 Paris, France
[c]CNRS, Institut des NanoSciences de Paris - UMR CNRS 7588, Université Pierre et Marie Curie - 4 place Jussieu, 75005 Paris, France
francois.coulouvrat@upmc.fr

Dispersion and absorption are examined for dilute suspensions of Ultrasound Contrast Agents of nanometric size (nUCA), with typical radii around 100 nm. This new generation of contrast agents is designed for targeted delivery of drugs. Compared to standard contrast agents used for imaging, particles are of smaller size to pass the endothelial barrier, their shell made up of biocompatible polymer (PLGA) is stiffer to undergo a longer time life and they have a liquid (PFOB) instead of a gaseous core. Ultrasound propagation in dilute suspension of nACUs is modelled by combining i) a dilatational mode of oscillation assuming an incompressible shell with a visco-elastic behaviour of Maxwell type (relaxation), and ii) a translational mode of oscillation induced by visco-inertial interaction with the ambient fluid. Experimental measurements of the dispersion and absorption properties of nACUs solutions over the 3-90 MHz frequency range are performed for various temperatures and concentrations. They allow to fit with good accuracy three unknown parameters of the nACUs shell : the thickness, the Young modulus and the viscosity (or equivalently the relaxation frequency). Obtained values are compatible with literature data and offer insight into the behaviour of PLGA shells in suspension (Work supported by programme Emergence-UPMC).

1 Introduction

A nanometric Ultrasound Contrast Agent (nUCA) is a new type of contrast agents currently investigated for nanomedicine applications, especially targeted drug delivery monitored by ultrasound [1, 2] or gene transfer. In the treatment of cancer, targeted chemotherapy would reduce both severe side effects and cell resistance. However, in comparison to standard UCA used for imaging, nUCA have to be multifunctional particles, simultaneously long-lasting ultrasound contrast agents and tumor-targeted drug carriers. They must be of nanometric size (radius less than 200 nm) to extravasate the large gaps between the endothelial cells of the anomalous vascularization of the tumor. They must have a sufficient life-time after intravenous administration to sustain pressure and mechanical stress and accumulate within the tumor. The proper choice of the (biocompatible) material for the particle shell is essential. The accumulation can be enhanced by decorating the shell with ligands targeting specific pathological tissues [3]. At low ultrasonic levels, particles must be sufficiently echogenic to be used as UCA. Higher ultrasound levels should be able to trigger drug delivery, either by breaking the particle shell, or by vaporizing the liquid core. Among the various types of nUCAs currently investigated, nanodroplets with a liquid perfluorocarbon (PFC) or perfluorooctyl bromide (PFOB) cores have interesting stability properties [4]. Even though they have much smaller echogenicity than microbubbles with a compressible gaseous core excited close to their resonance frequency, they can nevertheless be used for ultrasonic imaging. Biodegradable material for the shell can be a polymer like PLGA (poly(lactide-*co*-glycolide) acid), with surface phospholipids conjugated with polyethylene glycol (PEG) [5] in order to make it stealth to macrophages. For such materials, the ratio of the shell thickness to the total radius cannot be much smaller than 0.25. Recently, thinner shells were obtained by using Fluorinated TrisAcryl Conjugates (FTAC) instead of PLGA [6].

The acoustical behavior of suspensions of such nanodroplets with liquid cores remains mostly unexplored. Recent experiments [6] indicate increased echogenicity for thinner FTAC shells compared to thicker PLGA ones, and also a dramatic change of behavior between micrometric (a few microns) and nanometric (around 100 nm) sizes. Numerical simulations for micrometric objects [7] have been performed by neglecting viscous absorption effects. However, both viscous effects can be important in the acoustical properties of suspensions. For micrometric encapsulated bubbles, considering a volumic model [8] valid for an incompressible shell of finite thickness, shell viscosity has been shown to be one of the key parameters governing ultrasound absorption [9]. On the contrary, for rigid nanometric particles, visco-inertial translational effects are known to be dominant on ultrasound absorption [10, 11] and are easily measurable in the medical frequency range [12]. In the present situation of "large" nanometric droplets which are much less deformable than resonant micrometric bubbles, the question arises which mechanism is prevalent on the acoustical parameters of a dilute suspension: dilatational effects associated to the radial deformation of the viscoelastic shell, or translational effects associated to the visco-inertia of a quasi rigid particle embedded in a viscous fluid ? The objective of the present study is to answer that question.

2 Theoretical model

We consider a dilute suspension of nanometric contrast agents Fig.(1), composed of a spherical shell of inner radius R_1, outer radius $R_2 = R$ and thickness $h = R_2 - R_1$. The shell is assumed to be made of an incompressible, homogeneous and isotropic material. We assume in a first step the shell material satisfies a Kelvin-Voigt rheological behaviour:

$$\sigma = -p_S \mathbf{I} + \sigma^{ve} = -p_S \mathbf{I} + 2G_S \epsilon + 2\mu_S \dot{\epsilon}, \qquad (1)$$

where σ, σ^{ve} $\mathbf{I}$, ϵ and $\dot{\epsilon}$ are respectively the total stress, viscoelastic stress, unit, strain and rate of strain tensors. The material is characterized mechanically by its modulus of rigidity G_S and viscosity μ_S. The shell encapsulates a core fluid of density ρ_C and sound speed c_C. Active principles, if any, are located within that core. The particle volume is $V = 4\pi R^3/3$ and its mass is m_P. The ambient fluid is compressible and viscous, with specific mass ρ, sound speed c, shear viscosity μ and bulk viscosity ζ. Surface tension are respectively σ_1 for the shell / core interface, and σ_2 for the shell / ambient liquid interface. The volume concentration of the particles within the fluid suspension is Φ. For any quantity, index $_0$ designates its value at static equilibrium.

We use a multiphase homogeneous model with average balance equations of mass and momentum, assuming an acoustic wavelength much larger than the particle radius. For particles with radii around 100 nm, and acoustic frequencies in the biomedical range 1-100 MHz, the smallest wavelength is larger than 10 μm. Particles are assumed to be identical and randomly homogeneously distributed within the suspension. We note by p and $\mathbf{v}$ the mean pressure and velocity fields of the ambient fluid , and $\mathbf{v}_P$ the mean velocity field of the particles. The shell is impermeable : no mass exchange occurs between the particle and the ambient fluid. Thermal exchanges

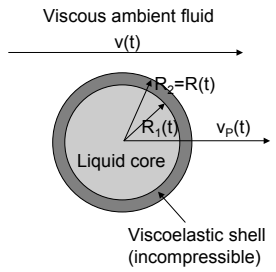

Figure 1: Particle geometry

due to a difference of temperature between the particles and the fluid are neglected. This is a well satisfied hypothesis for most liquid for which thermal effects are proportional to $\gamma-1$ where γ (the ratio of specific heats) is very close to 1. With all these assumptions, the average field satisfies the following balance equations of mass and momentum:

$$\frac{\partial}{\partial t}[(1-\Phi)\rho] + \nabla.[(1-\Phi)\rho\mathbf{v}] = 0 \quad (2)$$

$$\frac{\partial}{\partial t}[\Phi\rho_P] + \nabla.[\Phi\rho_P\mathbf{v}_P] = 0 \quad (3)$$

$$(1-\Phi)\rho\left[\frac{\partial \mathbf{v}}{\partial t} + (\mathbf{v}.\nabla)\mathbf{v}\right] - \nabla.\Sigma = -n\mathbf{f} \quad (4)$$

$$\Phi\rho_P\left[\frac{\partial \mathbf{v}_P}{\partial t} + (\mathbf{v}_P.\nabla)\mathbf{v}_P\right] = n\mathbf{f}. \quad (5)$$

One recognizes the usual mass (Eqs.(2-3)) and momentum (Eqs.(4-5)) balance equations for each fluid and particle phases, each phase being weighted by its volume fraction. In Eq.(4), Σ designates the stress tensor within the fluid phase. There is no source term in the mass equations because there is no mass exchange. Momentum exchanges are described by source terms with opposite signs because of action / reaction principle. In the dilute approximation, the total force undergone by a unit volume of the suspension is proportional to i) the number of particles per unit volume n, and ii) the force $\mathbf{f}$ exerted by the fluid on one single particle as if it were alone. Note that no coupling term is introduced in the present model, even though a volume variation can modify the particle translation [13]. However such coupling terms are nonlinear and are negligible in the linear acoustical regime. By noting that $\Phi = nV$ and $\rho_P = m_P/V$, Eq.(3) and Eq.(2) simplify into:

$$\rho_P V \partial n/\partial t = -\nabla.[\Phi\rho_P\mathbf{v}_P]. \quad (6)$$

$$(1-\Phi)\frac{\partial\rho}{\partial t} + \nabla.[(1-\Phi)\rho\mathbf{v}] = \rho n\frac{\partial V}{\partial t} - \frac{\rho}{\rho_P}\nabla.[\Phi\rho_P\mathbf{v}_P]. \quad (7)$$

For waves of sufficiently small amplitude, the linearized field equations are:

$$(1-\Phi_0)\left[\partial\rho/\partial t + \rho_0\nabla.\mathbf{v}\right] = \rho_0 n_0\partial V/\partial t - \rho_0\Phi_0\nabla.\mathbf{v}_P \quad (8)$$

$$(1-\Phi_0)\rho_0\partial\mathbf{v}/\partial t - \nabla.\Sigma = -n_0\mathbf{f} \quad (9)$$

$$m_P\partial\mathbf{v}_P/\partial t = \mathbf{f}. \quad (10)$$

For closure, these balance equations have to be completed by models describing the stress efforts Σ within the fluid, the evolution equation of the particle volume V and the force $\mathbf{f}$ exerted by the fluid on one single particle. The stress tensor is the one of a Newtonian viscous fluid characterized by its bulk (ζ) and shear (μ) viscosities. These ones may be modified by the presence of particles but, in the dilute case, they are almost identical to those of the pure fluid phase. Force exerted by the fluid phase on a single particle in the linear regime is given by the Faxen formula:

$$\mathbf{f} = 6\pi R\mu(\mathbf{v}-\mathbf{v_P}) + 6R^2\sqrt{\pi\rho\mu}\int_{-\infty}^{t}\frac{\partial}{\partial t'}(\mathbf{v}-\mathbf{v_P})\frac{dt'}{\sqrt{t-t'}} + \frac{2}{3}\pi R^3\rho\frac{\partial}{\partial t}(\mathbf{v}-\mathbf{v_P}) + \frac{4}{3}\pi R^3\rho\frac{\partial\mathbf{v}}{\partial t}. \quad (11)$$

In the above expression, the first term on the r.h.s. is Stokes viscous drag associated to a steady mismatch between the fluid and particles velocities. The second one is the so-called Basset-Boussinesq history force, taking into account the time delay between the flow motion and the particle response. The third one is the added mass effect, while the last one is the Archimede force associated to the mass of fluid displaced by the particle in an acceleration field. The first two terms are of viscous origin (proportional to the ambient fluid viscosity), while the last two ones are of inertial origin (proportional to the mass of fluid displaced by the particle). Above expressions are valid for a solid particle. Different expressions are used for instance for a bubble with a slip condition at the interface. We will see in the present case that the particle translational effects related to this force are significant only for relatively "stiff" particles with little volume changes. Hence, in case these effects are significant, the assumption of an almost rigid particle is indeed well satisfied. Note the three first terms on the r.h.s. are proportional to the velocity mismatch between the fluid and particle velocities, while Archimede force depends only on the fluid velocity.

Finally, the model is completed by the Church model [8] describing the motion of an incompressible viscoelastic spherical shell of finite thickness surrounded by a viscous liquid. The incompressible condition for the shell relates to one another the inner and outer radius $R_1^2\dot{R}_1 = R_2^2\dot{R}_2$. The radial motion of the shell is given by a generalized Rayleigh-Plesset equation (dot denotes time derivative):

$$\rho\left[(R_2\ddot{R}_2 + 1.5\dot{R}_2^2)\right] + \rho_S\left[(R_1\ddot{R}_1 + 1.5\dot{R}_1^2) - (R_2\ddot{R}_2 + 1.5\dot{R}_2^2)\right] = p_C(t) - p(t) - \frac{2\sigma_1}{R_1} - \frac{2\sigma_2}{R_2} - 4\mu\frac{\dot{R}_2}{R_2} - 4\mu_S\left(\frac{\dot{R}_1}{R_1} - \frac{\dot{R}_2}{R_2}\right) - 4G_S\left(1 - \frac{R_{1eq}}{R_1}\right)\left[1 - \left(\frac{R_1}{R_2}\right)^3\right]. \quad (12)$$

The first term on the l.h.s. describes the inertia of the ambient fluid. Compressible correction is here negligible. The second term is for the shell inertia. The first two terms on the r.h.s. are the pressure forces exerted by the inner (core) and outer ambient fluids. Both can be assumed to be spatially homogeneous because the particle radius is much smaller than the acoustic wavelength. The next two terms are the effects of the inner and outer surface tensions. Then come the outer fluid viscosity and the shell viscosity. The last term is the shell elasticity. Because particles are immersed within an ambient fluid, they may be in a pre-stressed state. Their actual static radius R_{10} may differ from their mechanical equilibrium radius R_{1eq}. This last one is easily computed by applying Eq.(12) in the static case. Note that Church model is obviously fully nonlinear. However, other strongly nonlinear mechanisms may occur for contrast agents like shell buckling or breaking [14]. As we will consider here only a linear behaviour, such effects can be ignored.

3 Dispersion relation

The dispersion relation for an acoustic wave propagating in such a medium can easily be obtained after linearization:

$$\left(\frac{k}{k_0}\right)^2 = \left(\frac{1-\Phi_0}{1-i(1-\Phi_0)\omega\tau_V\frac{1-D}{1+T}}\right)(1-D)\left(\frac{1+rT}{1+T}\right) \quad (13)$$

with $k_0 = \omega/c$ the wave number in the ambient fluid and:

$$\begin{aligned}
\epsilon &= h_0/R_{10} && (14)\\
A(\omega) &= -(4\pi/3)R_0^3\rho_0 i && (15)\\
B(\omega) &= 6\pi R_0\mu + 3\pi\sqrt{2\rho_0\mu\omega}R_0^2(1-i) + A/2 && (16)\\
\tau_V &= = (4\mu/3+\zeta)/(\rho_0 c^2) && (17)\\
r &= \rho_P/\rho_0 && (18)\\
T(\omega) &= \Phi_0/(1-\Phi_0)\times(B+A)/(B+rA) && (19)\\
D(\omega) &= \Phi_0/(1-\Phi_0)\times 3\rho_0 c^2/(R_0 C(\omega)). && (20)
\end{aligned}$$

Church model Eq.(12) yields a linear relation between applied pressure and particle radius with coefficient:

$$\begin{aligned}
C(\omega) &= \rho_0 R_0\omega^2\left(1+\frac{\rho_S}{\rho_0}\epsilon\right) - 3\rho_{C0}\frac{c_C^2}{R_0}(1+\epsilon)^3 \quad (21)\\
&+4i\frac{\omega}{R_0}\left(\mu+\mu_S((1+\epsilon)^3-1)\right) - \frac{2}{R_0^2}\left(\sigma_2+\sigma_1(1+\epsilon)^4\right)\\
&-4\frac{G_S}{R_0}\left((1+\epsilon)^3-1\right)\left[\frac{R_{1eq}}{R_{10}} - \frac{3}{(1+\epsilon)^3}\left(1-\frac{R_{1eq}}{R_{10}}\right)\right].
\end{aligned}$$

The geometrical parameter ϵ is the ratio of the shell thickness to its *inner* radius. Time τ_V measures bulk absorption of sound in the ambient fluid, while r is the ratio of the particle density to the ambient fluid density. Translational effects due to the viscous forces exerted on the particles (considered as almost rigid) are described by coefficient T. Dilatational effects due to the change of particle volume are described by coefficient D. In the dilute approximation, both of them are proportional to the particle volume fraction $\Phi_0 = n_0 V_0$. In the case of no particles ($\Phi_0 = T = D = 0$), and because in the considered frequency range $\omega\tau_V << 1$, one recovers the usual dispersion relation of a viscous fluid $k = k_0 + i\omega^2\tau_V/2c$. If bulk absorption is neglected ($\tau_V = 0$), there is no translational effect for particles of same density as the ambient fluid ($r = 1$). This is due to Archimede force. In particular, rigid particles of density equal to the ambient fluid oscillate in phase with this one.

If the shell is made up of a viscoelastic fluid which satisfies a rheological behaviour of the Maxwell type, one gets:

$$\sigma^{ve} + \tau_R\dot{\sigma}^{ve} = +2\mu_S\dot{\epsilon}. \quad (22)$$

with τ_R the relaxation time. At low frequencies, the shell material behaves as a viscous fluid and elastically at high frequencies. The low frequency viscosity μ_S and the high frequency rigidity modulus G_S are related by $G_S = \mu_S/\tau_R$. Indeed, PLGA is as a glassy polymer [15], a class of material exhibiting relaxation process(es) which are described in its most simple way by a Maxwell viscoelastic model . In that case, the model of Church can be modified [16]. Linearization yields the same expressions as for the Kelvin-Voigt case, except the expression for coefficient C which is now:

$$\begin{aligned}
C(\omega) &= \rho_0 R_0\omega^2\left(1+\tfrac{\rho_S}{\rho_0}\epsilon\right) - 3\rho_{C0}\tfrac{c_C^2}{R_0}(1+\epsilon)^3 \quad (23)\\
&+4i\tfrac{\omega}{R_0}\left(\mu+\tfrac{\mu_S}{1-i\omega\tau_R}((1+\epsilon)^3-1)\right) - \tfrac{2}{R_0^2}\left(\sigma_2+\sigma_1(1+\epsilon)^4\right).
\end{aligned}$$

4 Choice of a reference case

To quantify the relative importance of the various mechanisms, we consider a reference case. The ambient fluid (water) and liquid core (PFOB) have sound speeds equal to respectively 1500 m/s and 750 m/s, and densities equal to 1000 kg/m^3 and 1930 kg/m^3. The water shear viscosity μ is 1 $mPa.s$ and the bulk viscosity ζ is 2.41 $mPa.s$. The volume concentration of the nanodroplets is chosen equal to 1%, and the frequency range is the medical one 1-100 MHz.

The material of the nACU shell is PLGA (50 % PLA to PGA ratio - density 1350 kg/m^3). One outer radius R_0 = 75 nm will be examined, and the shell thickness chosen equal to 10% of the outer radius. Little is known about viscoelastic properties of the PLGA. A few experiments have been performed, with elastic moduli in the range 10 to 100 MPa [17]. A recent experiment using an atomic force microscope (AFM) [18] has shown that the Young modulus of polymer microspheres with nanometric thickness can be strongly dependent on the shell thickness, with about 1 order of magnitude variation (from 2 to 20 GPa) when the shell thickness decreases from 45 to 15 nm. Several possible explanations can be provided: a morphological and molecular restructuring of polymer chains under confinement, or an increased influence of surface tension and / or gradient elasticity. Given that uncertainty, it has been chosen here to perform a parametric study by varying the shell mechanical properties. In the reference case, we select a value $G_S = 60MPa$ and a shell viscosity $\mu_S = 1Pa.s$. For the Maxwell rheological model, this corresponds to a relaxation frequency $f_R = 1/(2\pi\tau_R) = 10MHz$. Note these values are typical for polymer-encapsulated air bubbles [9] and compatible with the few data on PLGA. Moreover, they give a shear wave velocity $c_T = \sqrt{G_S\rho_S} = 211m/s$, much smaller than measured compression wave velocities c_L [19] (in the range 1900 to 2400 m/s in the temperature range $[0-60°C]$, with a sharp transition at the glass transition), in agreement with the incompressible assumption.

For the selected values, one can estimate the magnitude order of various terms in the expression of $C(\omega)$ (unit Pa/m) for Kelvin-Voigt rheological model. Effects of core compressibility, surface tension and shell elasticity are independent of frequency. Core compressibility for PFOB gives a value about 7 10^{15} Pa/m. A liquid core has a very high impedance relative to gas, which strongly reduces the imaging contrast relative to gaseous microcapsules. The magnitude order of shell elasticity is slightly smaller, about 5 10^{14} Pa/m. For more rigid materials with higher modulus of rigidity (of the GPa order), it could however be comparable or even dominant. Hence shell elasticity has to be taken into account. Little is known about the value of surface tensions. As their effect is independent of frequency, it could be discriminated from the elastic one only by varying in a controlled way the radius of the particle while keeping the thickness ratio constant, something very difficult to perform at the nanometric scale. For the reference case and a "reasonable" interfacial tension of 0.1 $Pa.m$, one gets a contribution to C about 2 $10^{13}Pa/m$, about one or two orders of magnitude smaller than elasticity / core compressibility. Even though one cannot rule out they could play a significant role for smaller and thinner particles [18], they would anyway simply add to elasticity and contribute to an apparent increase of shell rigidity. For these reasons, we will assume here

$\sigma_1 = \sigma_2 = 0$. The static core and ambient liquid pressures are also chosen equal, so that the nanocapsule is initially not prestressed $R_{1eq} = R_{10}$. Inertia terms $\rho_0 R_0 \omega^2$ are negligible in all cases because of the small particle size. On the contrary, effects of shell viscosity are about $12\omega\mu_S\epsilon/R_0$, taking values 5 $10^{12} Pa/m$ at 1 MHz, 5 $10^{13} Pa/m$ at 10 MHz and 5 $10^{14} Pa/m$ at 100 MHz. Because of the chosen Kelvin-Voigt model, they increase linearly with frequency, and are comparable in order of magnitude to other mechanisms only at high frequencies. However, because they are the only non negligible term with an imaginary part, they will control the part of the absorption that emanates from dilatational effects, and are to be taken into account. On the contrary, influence of water viscosity is negligible.

5 Analysis of the reference case

Fig.(2) shows the sound velocity dispersion with frequency, and Fig.(3) the absorption coefficient (in dB/m) variation with frequency for particles with radius $R_0 = 75\ nm$. The absorption coefficient in the low frequency range ($0 - 20$ MHz) is zoomed on Fig.(4). Black lines display the overall effect. To identify the physical origin of the mechanisms of sound dispersion and absorption, magenta lines show the effect of water viscosity only ($D = T = 0$), red lines show the dilatational effects only ($T = \tau_V = 0$), and blue lines the translational effects ($D = \tau_V = 0$). When only dilatational / translational effects are considered, we label the absorption coefficient "D" or "T". For the dilatational and total effects, solid lines are for the Kelvin-Voigt model, and dashed ones for the Maxwell model. When water viscosity only is taken into account, one recovers the quadratic increase of absorption with frequency $Im(k) \approx \omega^2\tau_V/2c_0$. Note in this case the sound speed of the suspension $c_\phi \approx c_0/\sqrt{1-\Phi_0}$ is slightly increased (of about 0.5%, or 7.6 m/s) compared to pure water because of the presence of rigid particles that decreases its compressibility. On the contrary, taking into account particles change of radius (red lines) tends to decrease the sound speed because of the higher compressibility of PFOB relative to water. Considering shell viscosity, one can see that the "D" absorption coefficient is also independent on the particle radius, is proportional to shell viscosity and varies as the square of frequency for the Kelvin-Voigt model as is visible on red curves. On the contrary, that coefficient shows a strong dependence on capsules thickness. For the Maxwell model, the shell behaves quadratically with frequency as for the viscous case only for frequencies smaller than the relaxation frequency $f << f_R (= 10MHz)$. For higher frequencies, the "D" absorption coefficient tends to saturate as the medium behaves mostly as an elastic one. However, even in that case, because of the dependence of visco-elastic terms with $1/R_0$ in the expression of C, the related absorption coefficient remains independent on particle radius. Translational effects (blue lines) also induce some dispersion effects at low frequencies. A characteristic frequency is given by $f_T = \mu/(2\pi R_0^2 \rho_0)$, at which steady viscous Stokes drag and Basset-Boussinesq history force are of same amplitude. That frequency is equal here to about 28 MHz for particles of radius $R_0 = 75nm$. For frequencies much below f_T, the "T" absorption coefficient is proportional to the square of both the frequency and the particle radius. Such behavior can be observed on Fig.(4), with quadratic dependence of absorption with frequency up to about $f_T/3$ and larger translational absorption for larger particles at the same frequency. For frequencies much above f_T, an asymptotic expansion would lead to an absorption coefficient proportional to the square root of the frequency. However, such regime can be observed only when Archimede force is much higher that Basset-Boussinesq history force, e.g. for frequencies higher than $20 f_T$ that are out of the considered range. Hence, in the frequency range $[f_T - 20\ f_T]$, we are in an intermediate range where Stokes drag, Basset-Boussinesq history force, added mass effect and Archimede force are more or less of about the same order of magnitude. This gives a frequency dependence of the "T" absorption coefficient that is almost linear (in between power two and power half), and a weak dependence on radius.

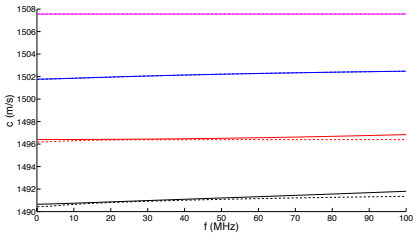

Figure 2: Sound velocity in the reference case. $R_0 = 75nm$. See text for colour code.

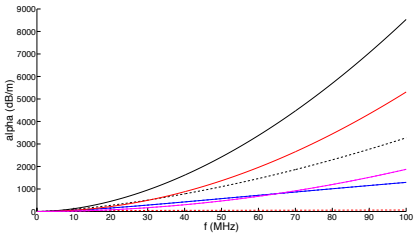

Figure 3: Sound absorption in the reference case. $R_0 = 75nm$. See text for colour code.

Concerning the absorption coefficient, the reference cases have been selected so that all effects are of the same order of magnitude. In the low frequency regime, one observes a quadratic dependence with frequency for all effects. As for sound speed, dependence with volume fraction is linear. Dilatational part is dependent on relative thickness and shell viscosity, while translational part is dependent on relative thickness and particle radius. For the considered radius $R_0 = 75\ nm$, the translational and dilatational parts are of the same order of magnitude in the low frequency regime 1-10 MHz. However, such hierarchy may be different for different materials depending on the effective value of the shell viscosity μ_S. In the high frequency regime, because translational effects are almost linear, dilatational effects and water bulk viscosity become dominant.

6 Preliminary experiments

Ultrasound pulse propagation is measured under thermal control in transmission in a cylindrical cell of varying length filled with the suspension. Nanocapsules are made of a PLGA-PEG shell encapsulating a PFOB liquid core [4]. Initial vol-

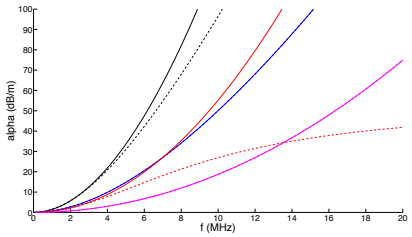

Figure 4: Zoom of Fig.(3) - frequency range 1-20 MHz

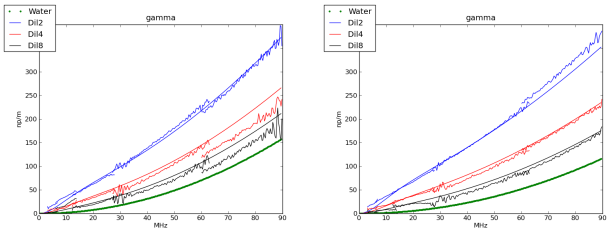

Figure 5: Measured and theoretical absorption coefficient of solutions of PLGA-PEG nUCA (diameter 100 nm - relative thickness 21%) in transmission versus frequency. Left 25°C. Right 37°C. Volume fraction : 0% (green) - 0.5 % (black) - 1% (red) - 2% (blue).

ume fraction of 2% is decreased after dilution. Mean diameter is estimated by Dynamic Light Scattering (DLS) or Transmission Electron Microscopy (TEM) to be around 100nm. Time windowed pulses are used to ensure free space propagation and get measurements independent of the cell boundaries. Repeated acquisition for several distances of propagation yields an absolute value of the phase velocity and attenuation. This technique removes indeterminacies in electronic or acoustic delays inherent to the design and set-up of transducers. The accuracy relies mainly on the precision of the length variation of the cell. This last parameter is presently controlled by a micrometer with manual linear stage.

On Fig.(5), we present a comparison between the above theoretical model (smooth solid lines) and a set of measurements (noisy solid lines) for the absorption coefficient and for three volume fractions (0.5% black, 1% red and 2% blue). The green curve is the attenuation of the pure liquid (water), and is presented as a reference case. Measurements are performed at two different temperatures (25°C and 37°C), showing significant differences in the viscoelastic properties of the PLGA-PEG shell. Mechanical properties of the shell (relative thickness, Young modulus and viscosity) are estimated through a best fit procedure between the model and the measurements. Maxwell relaxation model turns out to provide a better fit with measurements than the Kelvin-Voigt model. Relative thickness is estimated to be around 21%, in relatively good agreement with 25% thickness estimated from mass conservation assuming all products have reacted during the chemical reaction used for the particle synthesis. Best fit shows a sharp modification of the mechanical shell parameters from 25°C to 37°C. In the first case (25°C), shell viscosity is estimated to be 1.86 $Pa.s$ and Young modulus 1.65 GPa. In the second case, (37°C), shell viscosity is estimated to be 1.1 $Pa.s$ and Young modulus 0.2 GPa. This sharp softening of the material may indicate the temperature 37°C is not very far from the glass transition.

7 Acknowledgment

This work was performed within project NACUNAT (Nouveaux Agents de Contraste Ultrasonore Non-linéaires Appliqués à la Thérapie) supported by Université Pierre et Marie Curie - programme Emergence.

References

[1] N. Rapoport, Z. Gao, A. Kennedy, *J. Natl. Cancer Inst.* **99**, 1095-1106 (2007)

[2] N. Deshpande, A. Needles, J. K. Willmann, *Clinical Radiology* **65**, 567-581 (2010)

[3] D. Pan, G. Lanza, S. Wickline, S. C. Caruthers, *Eur. J. Radiology* **70**, 274-285 (2009)

[4] R. Diaz-Lopez, N. Tsapis, D. Libong *et al.*, *Biomaterials* **30**, 1462-1472 (2009)

[5] T. M. Fahmy, R. M. Samstein, C. C. Harness, W. M. Saltzman, *Biomaterials* **26**, 5727-5736 (2005)

[6] R. Berti, thèse de doctorat de l'Université Pierre et Marie Curie, Paris 6 (2011)

[7] G. Haiat, R. Berti, B. Galaz, N. Taulier, J.-J. Amman, W. Urbach, *J. Acoust. Soc. Am.* **129**, 1642-1652 (2011)

[8] C. C. Church, *J. Acoust. Soc. Am.* **97**, 1510-1521 (1995)

[9] L. Hoff, P. C. Sontum, J. M. Hovem, *J. Fluid Mech.* **107**, 2272-2280 (2000)

[10] M. Baudoin, J.-L. Thomas, F. Coulouvrat, D. Lhuillier, *J. Acoust. Soc. Am.* **121**, 3386-3397 (2007)

[11] M. Baudoin, J.-L. Thomas, F. Coulouvrat, *J. Acoust. Soc. Am.* **123**, 4127-4139 (2008)

[12] M. Baudoin, J.-L. Thomas, F. Coulouvrat, C. Chanéac, *J. Acoust. Soc. Am.* **129**, 1209-1220 (2011)

[13] J. Magnaudet, D. Legendre, *Phys. Fluids* **10**, 550-554 (1998)

[14] Ph. Marmottant, A. Bouakaz, N. de Jong, C. Quilliet, *J. Acoust. Soc. Am.* **129**, 1231-1239 (2011)

[15] K. van de Velde, P. Kiekens, *Polymer Testing* **21**, 432-442 (2002)

[16] A. A. Doinikov, P. A. Dayton, *J. Acoust. Soc. Am.* **121**, 3331-3340 (2007)

[17] A. Santovena, C. Álvarez-Lorenzo, A. Concheiro, M. Llabrés, J. B. Farina, *Biomaterials* **25**, 925-931 (2004)

[18] E. Glynos, V. Koutsos, W. N. McDicken *et al.*, *Langmuir* **25**, 7514-7522 (2009)

[19] N. G. Parker, M. L. Mather, S. P. Morgan, M. J. W. Povey, *Biomed. Mater.* **5**, 055005(1-10) (2010)